Available online at www.sciencedirect.com
SCIENCE DIRECT®
Journal of Magnetic Resonance 168 (2004) 124–131
JMR Journal of Magnetic Resonance
www.elsevier.com/locate/jmr

Resolution of ^{13}C–^{19}F interactions in the ^{13}C NMR of spinning solids and liquid crystals

Giancarlo Antonioli and Paul Hodgkinson*

Department of Chemistry, University of Durham, South Road, Durham DH1 3LE, UK

Received 16 December 2003; revised 6 February 2004

Abstract

Anomalous line-broadenings of carbon resonances close to ^{19}F have commonly been reported in the ^{13}C NMR of liquid crystals and solids. We have previously shown that these effects in static liquid-crystal samples are related to the difficulty of ^{1}H decoupling in the presence of strong ^{1}H–^{19}F dipolar interactions. We here extend this work to spinning samples (both liquid crystals and solids). A number of different line-broadening mechanisms are elucidated: analogous decoupling effects, magic angle misset, and ^{19}F lifetime-broadening. In relatively mobile systems, such as liquid crystals or soft solids, the limiting factor on ^{13}C resolution (and the ability to directly quantify the ^{13}C–^{19}F interactions) is found to be the efficiency and robustness of the ^{1}H-decoupling. In rigid solids, the lifetime of the ^{19}F spin-states is found to be an additional critical factor.

Keywords: Solid-state; Liquid crystal; NMR; Decoupling; ^{13}C; ^{13}F; Linewidth

1. Introduction

The presence of a single ^{19}F substituent would not be expected to have a significant effect on the ^{13}C NMR spectra of organic solids. Under the conditions of magic-angle spinning and ^{1}H decoupling, we would expect simple doublet patterns due to any resolved J_{CF} couplings. However, previous solid-state and liquid-crystal NMR studies of such systems have consistently remarked a significant line-broadening of resonances of the carbons close to a ^{19}F nucleus [1–4]. This line-broadening can be eliminated by ^{19}F decoupling, but this requires specialised equipment (due to the small fractional difference between ^{19}F and ^{1}H Larmor frequencies), and also results in the loss of information on the C–F interactions.

We recently observed these effects in the ^{13}C NMR of fluorine-containing liquid crystals and demonstrated that the broadening effects could be explained, at least in these systems, by the strong ^{1}H–^{19}F dipolar interactions effectively pushing nearby ^{1}H spins off resonance, thus degrading the efficiency of ^{1}H-decoupling [5]. The off-resonance effects are particularly severe for simple continuous-wave (CW) decoupling. Using more sophisticated decoupling schemes, most notably SPINAL-64 [6], we could obtain uniformly sharp linewidths across the full ^{13}C spectrum. Preliminary studies on relatively mobile solid systems suggested that analogous effects may be at work in the NMR of solid systems.

In this paper, we extend the previous work to spinning samples, considering initially spinning liquid-crystals. The molecular mobility of these samples reduces the magnitude of all anisotropic interactions and eliminates intermolecular couplings, leading to well-defined spin systems. We then consider rigid solid systems. Here, the magnitude of the various NMR interactions makes the analysis significantly more challenging.

2. Analysis

As previously shown [5], we can reproduce the essentials of the problem with a basic three spin system (^{13}C, ^{1}H, and ^{19}F). This has the Hamiltonian:

$$H = \delta_H(t)I_z^H + 2d_{HF}(t)I_z^H I_z^F + 2d_{CH}(t)I_z^C I_z^H + \delta_C(t)I_z^C + (2d_{CF}(t) + J_{CF})I_z^C I_z^F + H_{RF}(t), \quad (1)$$

* Corresponding author. Fax: +44-191-384-4737.
E-mail address: paul.hodgkinson@durham.ac.uk (P. Hodgkinson).

1090-7807/$ - see front matter © 2004 Elsevier Inc. All rights reserved.
doi:10.1016/j.jmr.2004.02.004

where d_{XY} represents the dipolar coupling between a pair of nuclei, δ_H, and δ_C are the offsets (shifts) of the ^1H and ^{13}C resonances from their transmitter frequencies, and H_{RF} is the time-dependent RF applied to the ^1H spins. The interactions are time-dependent due to the spinning of the sample. The offset of the ^{19}F from its transmitter frequency, δ_F, is omitted as it commutes with other terms. Only the ^{13}C–^{19}F J coupling, J_{CF}, is of interest; the other J couplings are neglected.

In the absence of ^{19}F RF irradiation, the ^{19}F spin quantum number is a good quantum number, and so the Hamiltonian can be block-diagonalised according to the ^{19}F spin state, i.e.,

$$H_{\alpha/\beta} = (\delta_H(t) \pm d_{HF}(t))I_z^H + 2d_{CH}(t)I_z^C I_z^H + (\delta_C(t) \pm [d_{CF}(t) + J_{CF}/2])I_z^C + H_{RF}(t). \quad (2)$$

The overall spectrum is the sum of sub-spectra associated with the different ^{19}F states: $S = S_\alpha + S_\beta$. The I_z^C term commutes with the other interactions, and so the α sub-spectrum, for example, is given by the convolution $S_\alpha = S_\alpha^\dagger \otimes S_\alpha^\ddagger$, where $S_\alpha^\dagger$ is the spectrum arising from the two-spin Hamiltonian

$$H_{\alpha/\beta}^\dagger = (\delta_H(t) \pm d_{HF}(t))I_z^H + 2d_{CH}(t)I_z^C I_z^H + H_{RF}(t) \quad (3)$$

and $S_\alpha^\ddagger$ the spectrum from the single-spin Hamiltonian

$$H_{\alpha/\beta}^\ddagger = (\delta_C(t) \pm [d_{CF}(t) + J_{CF}/2])I_z^C. \quad (4)$$

The $S^\ddagger$ are simply the ^{13}C spectra obtained in the limit of perfect ^1H decoupling (single lines at $\delta_C^{iso} \pm J_{CF}/2$ in the limit of fast spinning), while $S^\dagger$ are lineshape functions, dependent on the ^1H decoupling.

The three spin problem of Eq. (1) thus reduces to the effective two spin problem of Eq. (3), in which the additional ^{19}F simply modifies the effective ^1H offset, $\delta_H \to \delta_H \pm d_{HF}$. In the case of spinning samples, we must distinguish between the isotropic (time-independent) and anisotropic (time-dependent) components of δ_H (i.e., the isotropic shift and the CSA); d_{HF} will modify the effective CSA since it too transforms as a second rank tensor under sample rotation. While ^1H CSAs are correspondingly small, the dipolar couplings between spins of high magnetogyric ratio, such as ^1H and ^{19}F, can be considerable. This results in a substantial modification of the effective ^1H CSA.

The combination of non-negligible CSAs and dipolar interactions has surprising consequences on the effectiveness of decoupling. As shown theoretically and experimentally by Ernst et al. [7], this interaction can cause the linewidth of rare spin NMR spectra to dramatically *increase* under ^1H CW decoupling. These effects have been fully described in the literature [7,8] and the solution of Eq. (3) is not repeated here. The key point is that the combination of RF irradiation, and the two time-dependent rank 2 interactions (dipolar couplings and CSAs) results in rank 4 cross-terms which are not eliminated by magic-angle spinning (cf. second-order quadrupolar interactions). In mild cases, the consequence is simply an unwanted line-broadening, while in more severe cases, the separate ^1H spin states are resolved leading to a broad double-peaked powder pattern. If restricted to CW decoupling, this line-broadening is only removed in the limit of prohibitively large RF decoupling strengths. However, suitable phase-alternated decoupling can strongly reduce or even eliminate these effects [7].

These effects are illustrated for the ^{13}C–^{19}F–^1H spin system in the simulations of Fig. 1. In the absence of significant ^1H CSA Fig. 1A, a simple doublet split by the J_{CF} coupling is observed. A significant CSA causes each component of the doublet to broaden into a double-peaked lineshape as a result of the interaction between the CSA, d_{CH} coupling, and CW decoupling. ^1H CSAs are normally too small for these effects to be observed

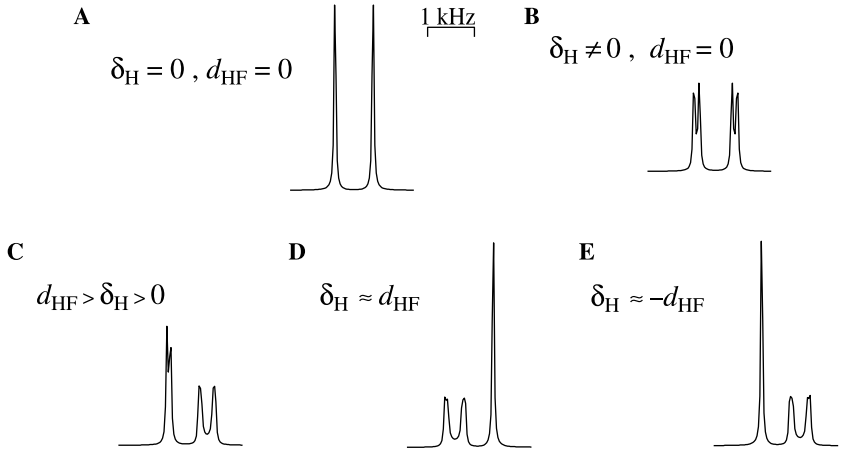

Fig. 1. Simulations of the CW-^1H-decoupled ^{13}C spectrum in a ^{13}C–^{19}F–^1H system under MAS for different combinations of the chemical shift anisotropy, δ_H and ^1H–^{19}F dipolar coupling, d_{HF}: (A) $\delta_H = d_{HF} = 0$, (B) non-zero CSA, $d_{HF} = 0$, (C–E) non-zero CSA and H–F coupling. Only the centreband is shown.

routinely in $\{^1H\}$–^{13}C NMR. A non-zero d_{HF} coupling Fig. 1C–E, however, significantly modifies the effective CSA. The effects are asymmetrical, depending on the relative signs of δ_H and d_{HF}. This is entirely analogous to the behaviour previously observed in static liquid crystals [5].

3. Spinning liquid crystals

Liquid crystals are a useful staging post between solution-state NMR (all anisotropic interactions eliminated by molecular tumbling) and solid-state NMR (multiple inter- and intramolecular interactions present). Rapid, but anisotropic, re-orientation in liquid crystals eliminates intermolecular couplings, while intramolecular anisotropic interactions are reduced to their projection along the director axis of the local domain (in the case of uniaxial nematic phases).

Liquid crystal samples may be spun in order to reproduce the effect of magic-angle spinning on solids. The fluid dynamics are not entirely straightforward, as they depend on the interplay between the spinning and the aligning effect of the field [9]. Roughly speaking, however, we expect local directors in samples spinning about an axis away from the magic angle to become aligned along or perpendicular to the spinning axis (depending on relative signs of the anisotropy of the bulk magnetic susceptibility, $\Delta\chi$, and $P_2(\cos\theta)$, where θ is the angle of the rotation axis relative to the magnetic field axis). Exactly at the magic angle, there is no net aligning torque and the local directors should be randomly oriented (as in a powdered solid sample). The presence of spinning sidebands is a useful check that the entire sample is spinning and is not simply being aligned by the spinning. A liquid crystal sample spinning at the magic angle should thus be a good model for the NMR of powdered solids, but without the degradation of resolution caused by the intermolecular interactions present in genuine solids.

As in our previous study, we have studied the ^{13}C NMR of the liquid-crystal I35 (molecular structure given in Fig. 2). The ^{13}C–^{19}F dipolar interaction will be modulated by the sample spinning, and so give rise to spinning sidebands or be suppressed entirely. Hence, the ^{13}C resonances will simply be split by any resolved ^{13}C–^{19}F J couplings.

Fig. 2 shows a series of ^{13}C NMR spectra (50.32 MHz for ^{13}C) of I35 spinning at the magic angle. The sample was retained in 7.5 mm o.d. rotors (Varian/Chemagnetics, CO) by a tight-fitting PTFE spacer. A spinning speed of 2.8 kHz was sufficient to avoid spinning sidebands, without causing significant frictional heating or pressures that would have strained these basic sample sealing arrangements. TPPM decoupling [10] is used to illustrate the effects of the decoupling sequence on spectral resolution. In addition to the RF field strength, TPPM has two parameters: the phase difference between the successive pulses, $\Delta\phi$, fixed, after initial optimisation, at 14°, and the pulse nutation angle, β. As can be

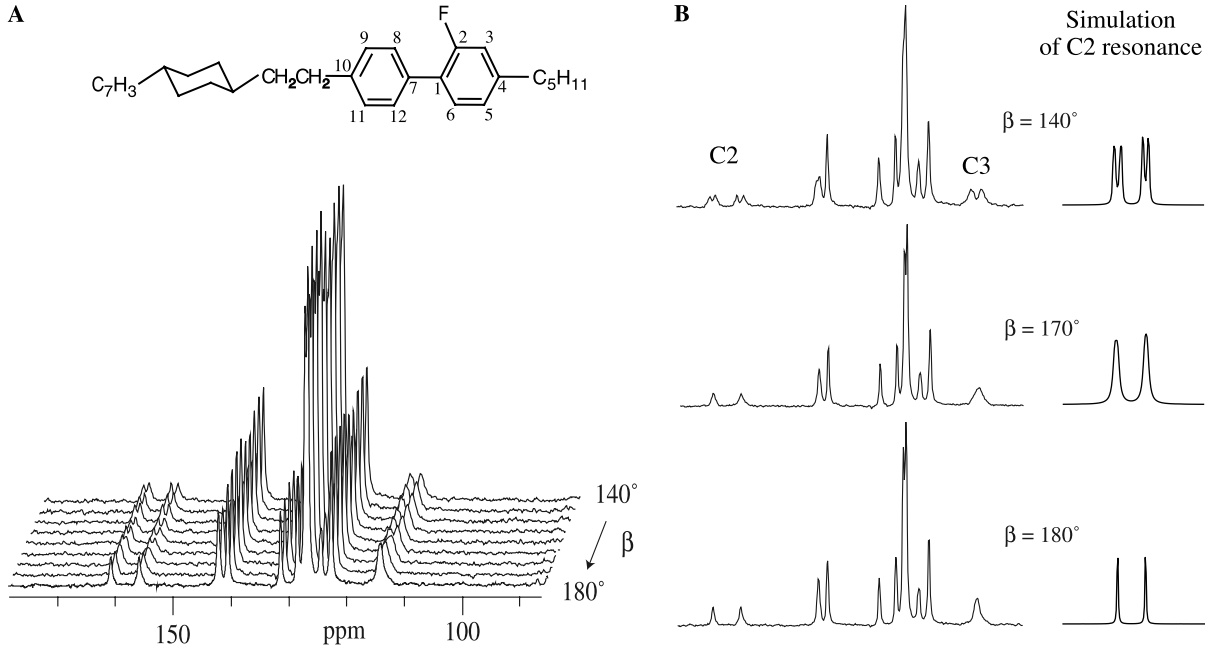

Fig. 2. (A) ^{13}C MAS NMR spectra of I35 using TPPM ^1H decoupling as a function of the TPPM tip angle (phase difference fixed at 14°), with $\nu_{rf} = 50$ kHz, $\nu_r = 2.8$ kHz. (B) Comparison of selected slices with simulation of the C2 doublet, using the experimental values for spinning speed and decoupling parameters, and estimates of 1 and 8 kHz for the motionally-averaged ^1H CSA and ^{13}C–^1H dipolar interaction, respectively.

clearly seen in the figure, the resolution of the ^{13}C resonances in proximity to the ^{19}F is strongly dependent on the value of β. The resolution is optimal for a β angle of exactly π radians, in line with earlier predictions [7]. At different β angles, the effective CSA/dipolar coupling interference results in severe broadening and eventual separation into a crude "doublet." The simulated spectra on the right of the figure have been calculated using estimated values for the various NMR parameters involved, and confirm that the observed dependence on the TPPM tip angle can be satisfactorily described in terms of this simple three spin model.

The TPPM tip angle, β, was varied at a fixed $\Delta\phi$ in Fig. 2 primarily to verify that the observed effects are reproduced by the proposed model, but the optimal value of β also has significance. The optimal values of β in conventional applications of TPPM (typically 160–170° [10]) are consistently smaller than $\beta = 180°$ predicted from a two spin model of ^{1}H decoupling and CSA/dipolar interference. In this case, however, where the resolution of some sites is clearly limited by these effects, the optimal value of β is indeed 180°. In static samples of I35 (where the overall resolution is somewhat better), we find the optimal value of β for "ordinary" sites is about 165°. This difference in optimal decoupling conditions strongly indicates that CSA/dipolar interference is unlikely to be a primary factor in determining the performance of ^{1}H decoupling sequences, and, by implication, that two spin models are probably inadequate to describe ^{1}H decoupling in strongly coupled systems. It is perhaps significant that the most effective decoupling sequences have been devised largely empirically [6] or by "direct optimisation" [11], rather than from theoretical models based on limited spin systems.

Fig. 3 shows a comparison of the aromatic region of ^{13}C MAS spectra of I35 under optimised CW, TPPM, and SPINAL-64. The resolution in the alkyl region of the spectra is not measurably affected by changes in decoupling and limited by factors such as B_0 inhomogeneity and RF heating. However, in the aromatic region, where the effects of the ^{19}F are strongest, the resolution clearly improves on changing the decoupling from CW to TPPM, and better still SPINAL-64, which is consistent with previous results on static samples and soft solids [5].

4. Spinning solids

It could be argued that spinning liquid crystals represent a rather particular and unrepresentative case. In common with the soft solid systems on which these effects have also been demonstrated, all components of the anisotropic interactions perpendicular to the director (or crystal) axis have been averaged away. As a consequence, the motionally averaged anisotropic interactions share a common principal axis system defined by the director axis, and so have the same time dependence when subject to macroscopic rotation. By definition, such a Hamiltonian commutes with itself at all times and so is "inhomogeneous" in the sense defined by Maricq and Waugh [12]. The spectra of such systems readily break up into sharp spinning sidebands under magic angle spinning. In "real" solids, however, the anisotropic interactions do not share a principal axis system and the overall Hamiltonian does not commute with itself at different times, resulting in sidebands with a distinct width that decreases relatively slowly with increasing spin rate.

As a result, it is important to also evaluate the influence of strong ^{1}H–^{19}F interactions on conventional rigid solids. Fig. 4 shows the results of varying the ^{1}H decoupling on the ^{13}C spectra of flurbiprofen, a molecule which contains the same F-substituted biphenyl motif as I35 (structure shown in the figure). There is no significant improvement in resolution across most of the spectrum on switching to TPPM decoupling, which is typical for this modest spin-rate (5 kHz) and magnetic

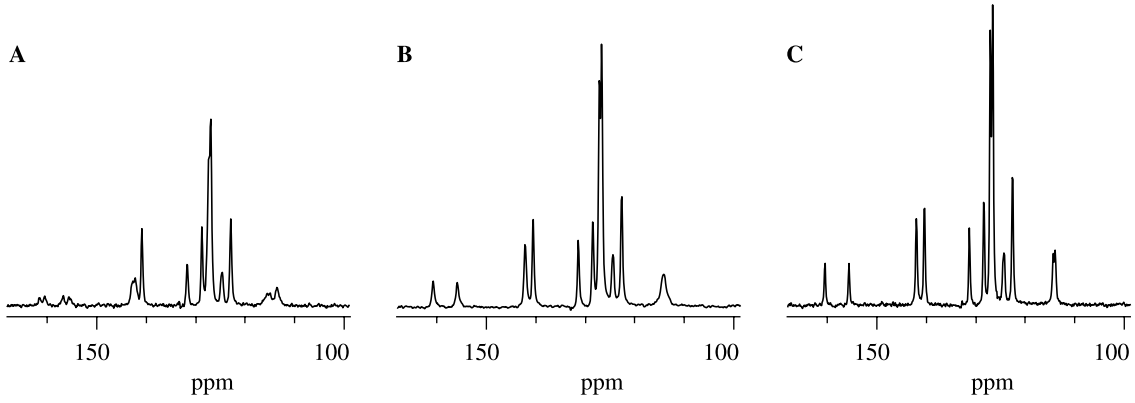

Fig. 3. Aromatic region of ^{13}C MAS NMR spectra of I35 as a function of decoupling method: (A) CW, (B) TPPM, and (C) SPINAL-64, with $\nu_{rf} = 50$ kHz, $\nu_r = 2.8$ kHz. 180° tip pulses were optimal for both TPPM and SPINAL-64 decoupling.

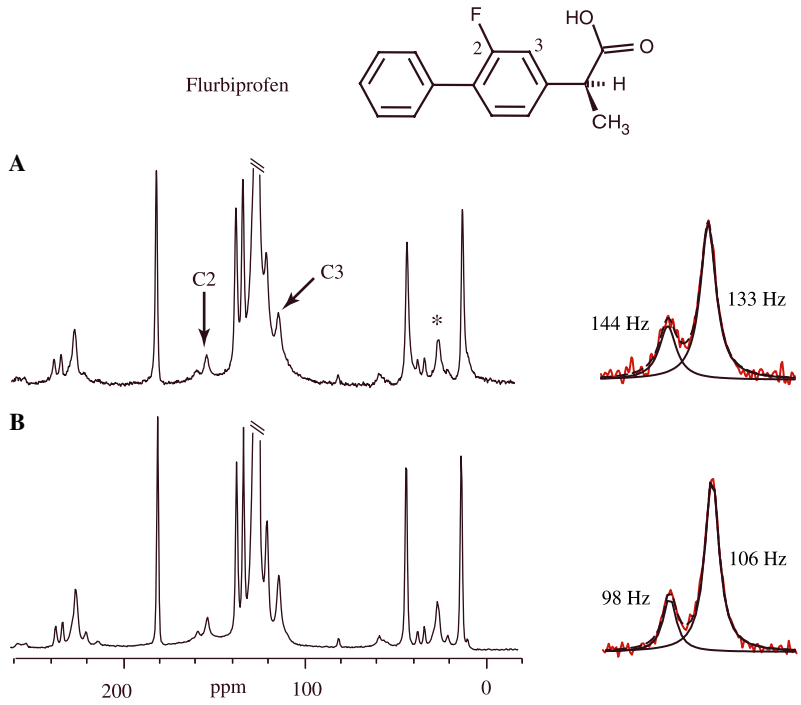

Fig. 4. CP/MAS ^{13}C spectra of flurbiprofen using 50 kHz (A) CW and (B) TPPM ^{1}H-decoupling. Expansions show the fit of the two components of the J_{CF} doublet of C2 to Lorentzian lineshapes (the numbers are the fitted FWHM linewidths). Acquisition parameters: spinning speed 5 kHz, cross-polarisation contact time 3 ms, and recycle delay 15 s.

field (4.7 T). In contrast, the resolution of the C3 peak is significantly improved, as we would predict. The overall resolution is still relatively poor in this sample, but this would appear to be a sample issue. The linewidths (of peaks unaffected by ^{19}F interactions) in the spectrum at a ^{13}C Larmor frequency of 125.7 MHz were generally a factor of three larger than those at 50.3 MHz (60–80 Hz), implying that the linewidth is essentially "inhomogeneous" (not to be confused with the inhomogeneous character or otherwise of the *Hamiltonian*). These linewidths were unchanged after careful re-crystallisation of the sample, suggesting that the broad lines are a consequence of a large $\Delta\chi$ (anisotropy of the bulk magnetic susceptibility—ABMS) for this compound [13]; a likely common feature of systems with this fluorobiphenyl motif.

In contrast to the marked resolution improvements observed for C3, the expected J_{CF} doublet from C2 is poorly resolved and strongly distorted; a situation which seems to be little improved by more sophisticated decoupling. In part, this is due to the large inhomogeneous linewidth obscuring modest linewidth improvements. Subtracting an estimated inhomogeneous linewidth of 70 Hz shows that the homogeneous linewidth has decreased by a factor of about two. Nevertheless, the intensity and resolution of the doublet is poor in comparison to the rest of the spectrum.

The distortion of the expected symmetrical doublet can be explained in terms of effects that have been previously observed in different contexts. The unequal intensity of the two components of the doublet is a consequence of the interaction between tensor interactions [14]. If we consider an isolated ^{13}C–^{19}F system, then the sideband pattern observed in the ^{13}C spectrum will involve both the ^{13}C CSA and the ^{13}C–^{19}F dipolar interactions. In the presence of a resolved J-coupling, we will see two distinct sideband manifolds corresponding to the two ^{19}F spin states. These sideband manifolds will be different. In one manifold, the two anisotropies will tend to add constructively, resulting in a wide sideband pattern and a correspondingly reduced intensity in the individual sidebands. While in the other manifold, the interactions will partly cancel, resulting in fewer spinning sidebands with correspondingly greater intensity.

This is illustrated in the simulations of Fig. 5. At spinning speeds lower than the effective anisotropies, Fig. 5A, the differences between the spinning sideband manifolds associated with the different X spin states (α and β) are marked, resulting in very different centreband intensities. At higher spinning speeds, Fig. 5B, the signal intensity is concentrated in the centreband and the effects of the different effective anisotropies are less marked. Obviously, a simple symmetrical J doublet will be seen in the limit of spinning much faster than the anisotropies. This effect readily accounts for the asymmetrical intensity of the C2 doublets observed in Fig. 4.

The large effective anisotropy of one component of the C2 doublet makes it particularly sensitive to the

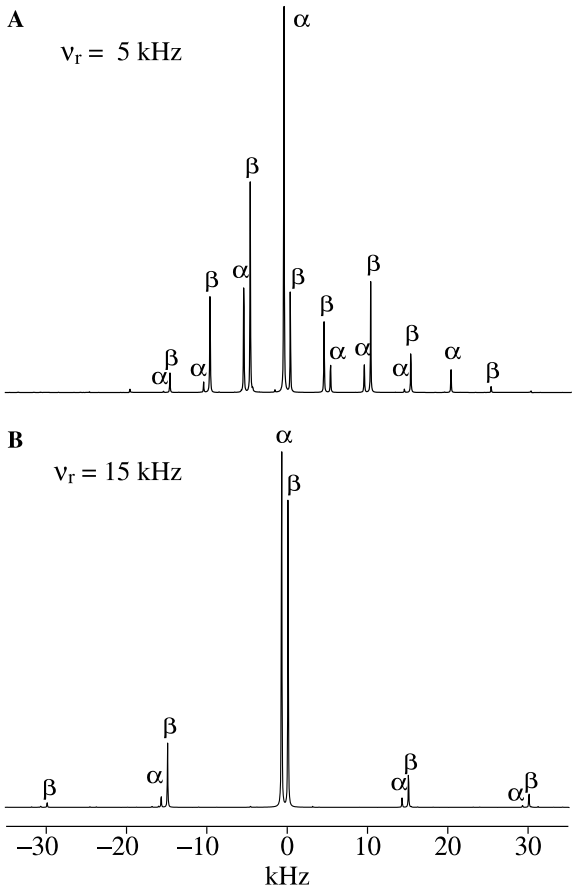

Fig. 5. Simulation of the ^{13}C spinning sideband pattern in a C–H–X system at spinning speeds of 15 kHz (B) and 5 kHz (A) using 50 kHz TPPM decoupling (with $\beta = 180°, \Delta\phi = 14°$). Other simulation parameters: ^{1}H CSA of 2 kHz, ^{13}C CSA of 15 kHz, $d_{HX} = 6$ kHz, $d_{CH} = 8$ kHz, $d_{CX} = 4$ kHz, and $J_{CX} = 800$ Hz (tensor quantities are co-linear).

setting of the magic angle. If the spinning axis deviates from the magic angle, then the underlying lineshapes become scaled powder patterns. The extent of the resulting line-broadening is proportional to the anisotropy involved, and so in this situation of very different effective anistropies, a misadjustment of the magic angle results in a differential line-broadening of the doublet components. This can be seen in Fig. 6 which shows the results of fitting the J doublet components. In the off-angle spectrum Fig. 6A, the components have different linewidths and the frequency separation (not simply the peak-to-peak splitting) is markedly smaller than expected values of $^{1}J_{CF}$ [15]. The very large effective CSA resulting from the H–F interaction has shown up a minor misadjustment of the magic angle which may otherwise have gone unnoticed. Apart from degrading the resolution, the introduction of asymmetrical lineshapes in this way will distort measurements of the J coupling [16]. Note how the nature of the line-broadening is not apparent at this resolution; it is only the asymmetry in the linewidths which raises suspicions. In contrast, the doublet obtained after re-calibration of the magic angle (from the rotor echoes of KBr), Fig. 6B, has essentially equal linewidths and the splitting is now a reasonable measure of $^{1}J_{CF}$.

5. Resolution of ^{13}C–^{19}F interactions in liquid crystals and solids

Although faster magic-angle spinning (reducing the loss of centreband intensity into spinning sidebands) and appropriate ^{1}H decoupling (countering the perturbing effects of strong ^{1}H–^{19}F dipolar interactions) together significantly improve the resolution of the ^{13}C–^{19}F interactions, the resolution of sites closest to the ^{19}F is still disappointing. This contrasts with the situation in spinning liquid crystals (above) and soft solids [5] where essentially uniform resolution can be obtained across the spectrum.

The final component to this problem is the effect of the finite lifetime of the ^{19}F spin states on the ^{13}C spectrum. If the "relaxation rate" of the ^{19}F is fast compared to the size of the coupling, then a single line will be observed in the ^{13}C spectrum; the ^{19}F is said to be

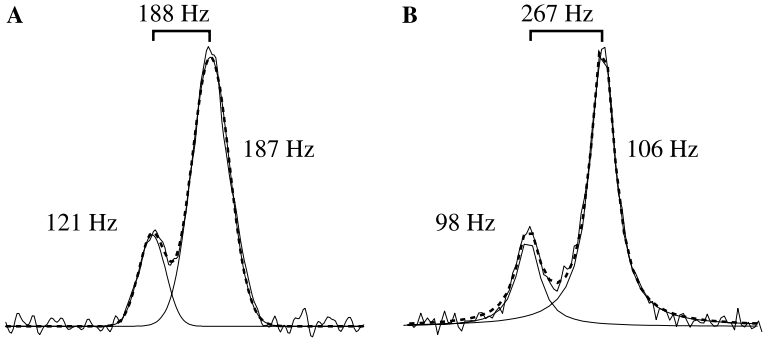

Fig. 6. Fitting of the J_{CF} doublet of the ^{13}C CPMAS spectrum of flurbiprofen (A) slightly off and (B) exactly on the magic angle. Figures show linewidths and separation of fitted Gaussian and Lorenztian lineshapes, respectively. Acquisition parameters: $\nu_r = 5$ kHz, contact time 3 ms, and recycle delay 15 s, TPPM decoupling with $\nu_{rf} = 50$ kHz, $\beta = 180°, \Delta\phi = 14°$.

"self-decoupled." A smaller, but non-negligible, relaxation rate will cause line-broadening of the J doublet. This effect is well-known from the solution state, usually in the context of quadrupolar nuclei [17,18], where relaxation is rapid, but also for coupling between spin-1/2 nuclei [19]. The nature of spin state lifetimes in the solid-state is less clear cut since these are dominated by coherent effects ("spin diffusion" due to multiple dipolar couplings) rather than truly incoherent relaxation. Some insight into this problem is provided by earlier work considering the ^{13}C spectrum of adamantane under fast magic-angle spinning [20]. Given sufficiently fast MAS, it should be possible to resolve J multiplets in the simple "undecoupled" ^{13}C spectrum, but this was not observed even at the highest spinning speeds used. This can be rationalised in terms of persisting spin-diffusion between the protons preventing resolution of the J couplings, and the experimental results modelled using exchange-modified Bloch equations, the spectrum being determined by diagonalising the spectral matrix

$$\begin{pmatrix} -k - i\pi J & k \\ k & -k + i\pi J \end{pmatrix}, \tag{5}$$

where k is the rate of "exchange" between the α and β states. The imaginary part of the eigenvalues give the line positions (angular frequency units), and the real parts the decay rate.

The same spectral matrix applies to both the "exchanging" spin (in our case ^{19}F) and the spin to which it is coupled, i.e., the linewidth of the components of the J doublet in the ^{13}C spectrum should be more or less equal to the linewidth in the ^{19}F spectrum. Hence, we can estimate k from the homogeneous linewidth of ^{19}F as determined from a Carr–Purcell or spin-echo measurement of its "T_2." For flurbiprofen, the simple spin-echo measurement results fit to a single exponential with a time constant of $630 \pm 30\,\mu s$. (A Carr–Purcell train would allow the data to be collected in a single shot, but we have noticed anomalous behaviour when applying such pulse trains to dipolar coupled systems.) A corresponding measurement on the I35 sample, under the same conditions as Fig. 2, gave a value of 41 ± 1 ms.

The difference of two orders of magnitude in the "T_2" in these two systems is large, but it is consistent with the difference in linewidth in their simple ^{19}F spectra (24 and 1280 Hz, respectively) and goes a long way to explaining the difference in resolution of the ^{13}C–^{19}F interactions. The T_2 of 45 ms (corresponding to a k of 22 Hz) puts the spinning liquid crystal firmly into the limit of $k \ll 2\pi J$, i.e., little broadening of the doublet due to the ^{19}F lifetime. By contrast, the much shorter value of "T_2" in flurbiprofen places it in the $k \sim 2\pi J$ regime, where the J coupling is on the limits of resolution. Although quantitative comparisons are suspect due to the simplistic nature of this model of an intrinsically multi-spin problem, this is consistent with the experimental data. The ability to resolve the ^{13}C–^{19}F interactions is clearly linked to the question of ^{19}F linewidth.

6. Conclusion and discussion

As concluded from the earlier study on liquid crystal samples [5], the ability to resolve, and hence quantify, ^{13}C–^{19}F interactions in the ^{13}C NMR of spinning samples depends critically on the efficiency of the heteronuclear ^{1}H decoupling. This needs to be robust with respect to the perturbing effect of the strong ^{1}H–^{19}F dipolar couplings. For samples subject to magic-angle spinning, these dipolar couplings behave as large effective ^{1}H shift anisotropies, greatly amplifying the interference between the effective ^{1}H CSA and ^{13}C–^{1}H dipolar interaction under continuous wave decoupling—an effect which is not normally apparent due to the small size of ^{1}H CSAs. As predicted, simple phase-alternated decoupling schemes greatly reduce this effect, and more sophisticated schemes such as SPINAL64 work better still. Differences in the effective ^{13}C CSA (due to the ^{13}C–^{19}F dipolar interaction) often cause the expected doublet from the $^{1}J_{CF}$ interaction to be asymmetrical, due to the different intensity distribution in the spinning sideband manifolds from the two ^{19}F spin states. Linewidths in the doublets and the apparent. Misset of the magic angle result in asymmetric broadenings of the doublet components, which degrades resolution and compromises the quantification of the J_{CF} interactions.

Unlike the liquid crystal samples, however, the resolution of the J couplings in solid samples is not usually limited by the decoupling efficiency, but by the lifetime of ^{19}F spin states. If $J < 1/2\pi T_2$ (^{19}F), then the J doublet is unlikely to be resolved in the ^{13}C spectrum. This is often the case in rigid solids, which explains the difficulties that previous workers have encountered in trying to observe these interactions. While the resolution in soft solids and liquid crystals is highly sensitive to the decoupling [5], the resolution in the systems studied was relatively insensitive to variations of the decoupling sequence (e.g., TPPM vs. SPINAL64).

Resolving ^{13}C–^{19}F interactions in C–H–F spin systems may seem a rather obscure problem in NMR spin dynamics. There are, however, a couple of more general insights provided by this work. First, it provides clues to the nature of heteronuclear decoupling in organic solids under MAS. This subject has taken on particular importance with the realisation that the resolution and sensitivity in many important classes of ^{13}C NMR experiments is limited by the purely homogeneous linewidth, which is dominated by the effects of imperfect ^{1}H decoupling [21]. It has been suggested that the interaction between the chemical shift anisotropy and dipolar interaction under MAS forms the major

component to proton-decoupled ^{13}C linewidths in solid-state NMR [8]. The observation in these systems that the optimal conditions for decoupling protons strongly affected by this specific mechanism (i.e., those close to ^{19}F) are different from those required for optimal decoupling of "normal" protons, suggests that this is far from being the complete picture. So, while limited spin models can explain this specific line-broadening mechanism, a fuller understanding of decoupling is likely to require a more complete treatment of the strong homonuclear dipolar coupling network between the protons.

The other question indirectly addressed in this work is that of ^{19}F resolution in the solid-state. ^{19}F resonances in solid samples are generally surprisingly broad. For example, in the flurbiprofen sample, the SPINAL64-^{1}H-decoupled ^{19}F MAS spectrum shows a single line of width 685 Hz (spin rate 6 kHz), which is about an order of magnitude larger than the ^{13}C resonances under the same conditions (this difference would be even greater if the effects of inhomogeneous broadening were to be subtracted). It is certainly much greater than the ratio $\gamma(^{19}F)/\gamma(^{13}C) = 3.7$ which we could reasonably expect for these "rare-spin" systems if the linewidth were controlled by classic relaxation mechanisms. Work to better understand the nature of ^{19}F linewidths in solids is currently in progress. This in turn should allow us to improve the resolution of ^{13}C resonances in proximity of ^{19}F.

References

[1] E.W. Hagaman, ^{13}C–^{19}F dipolar dephasing in monofluorinated organic substances. Characterization by ^{1}H–^{13}C–^{19}F triple-resonance ^{13}C CP/MAS and ^{19}F MAS NMR, J. Magn. Reson. Ser. A 104 (1993) 125–131.

[2] A. Nordon, R.K. Harris, L. Yeo, K.D.M. Harris, Application of triple-channel $^{13}C\{^{1}H,^{19}F\}$ NMR techniques to probe structural properties of disordered solids, Chem. Commun. 21 (1997) 2045–2046.

[3] R.K. Harris, A. Nordon, K.D.M. Harris, Ring inversion of fluorocyclohexane in its solid thiourea inclusion compound, Magn. Reson. Chem. 37 (1999) 15–24.

[4] E. Ciampi, M.I.C. Furby, L. Brennan, J.W. Emsley, A. Lesage, L. Emsley, The structure, conformation and orientational order of fluorinated liquid crystals determined from carbon-13 NMR spectroscopy, Liq. Cryst. 26 (1) (1999) 109–125.

[5] G. Antonioli, D.E. McMillan, P. Hodgkinson, Line-splitting and broadening effects from ^{19}F in the ^{13}C NMR of liquid crystals and solids, Chem. Phys. Lett. 344 (2001) 68–74.

[6] B.M. Fung, A.K. Khitrin, K. Ermolaev, An improved broadband decoupling sequence for liquid crystals and solids, J. Magn. Reson. 142 (2000) 97–101.

[7] M. Ernst, S. Bush, A.C. Kolbert, A. Pines, Second-order recoupling of chemical-shielding and dipolar-coupling tensors under spin decoupling in solid-state NMR, J. Chem. Phys. 105 (1996) 3387–3397.

[8] M. Ernst, Heteronuclear spin decoupling in solid-state NMR under magic-angle sample spinning, J. Magn. Reson. 162 (2003) 1–34.

[9] J. Courtieu, J.P. Bayle, B.M. Fung, Variable-angle sample-spinning NMR in liquid crystals, Prog. Nucl. Magn. Reson. Spectrosc. 26 (2) (1994) 141–169.

[10] A.E. Bennett, C.M. Rienstra, M. Auger, K.V. Lakshmi, R.G. Griffin, Heteronuclear decoupling in rotating solids, J. Chem. Phys. 103 (16) (1995) 6951–6958.

[11] G. de Paëpe, P. Hodgkinson, L. Emsley, Improved heteronuclear decoupling schemes for solid-state magic angle spinning NMR by direct spectral optimization, Chem. Phys. Lett. 376 (3–4) (2003) 259–267.

[12] M.M. Maricq, J.S. Waugh, NMR in rotating solids, J. Chem. Phys. 70 (7) (1979) 3300–3316.

[13] D.L. VanderHart, W.L. Earl, A.N. Garroway, Resolution in ^{13}C NMR of organic solids using high-power proton decoupling and magic-angle sample spinning, J. Magn. Reson. 44 (1981) 361–401.

[14] R.K. Harris, K.J. Packer, A.M. Thayer, Slow magic-angle rotation ^{13}C NMR studies of solid phosphonium iodides. The interplay of dipolar, shielding, and indirect coupling tensors, J. Magn. Reson. 62 (1985) 284–297.

[15] J.W. Emsley, L. Phillips, V. Wray, Fluorine Coupling Constants, Pergamon Press, 1977.

[16] T. Terao, H. Miura, A. Saika, Dipolar SASS NMR spectroscopy: separation of heteronuclear dipolar powder patterns in rotating solids, J. Chem. Phys. 85 (7) (1986) 3816–3826.

[17] J.A. Pople, The effect of quadrupole relaxation on nuclear magnetic resonance multiplets, Mol. Phys. 1 (1958) 168–174.

[18] M. Suzuki, R. Kubo, Theoretical calculation of NMR spectral line shapes, Mol. Phys. 7 (1963) 201–209.

[19] H.S. Gutowsky, D.W. McCall, C.P. Slichter, Nuclear magnetic resonance multiplets in liquids, J. Chem. Phys. 21 (2) (1953) 279–292.

[20] M. Ernst, A. Verhoeven, B.H. Meier, High-speed magic-angle spinning ^{13}C MAS NMR spectra of adamantane: self-decoupling of the heteronuclear scalar interaction and proton spin diffusion, J. Magn. Reson. 130 (1998) 176–185.

[21] D. Sakellariou, S.P. Brown, A. Lesage, S. Hediger, M. Bardet, C.A. Meriles, A. Pines, L. Emsley, High-resolution NMR correlation spectra of disordered solids, J. Am. Chem. Soc. 125 (14) (2003) 4376–4380.